

doi:10.15199/48.2023.07.46

## Research of pressure losses and justification of forms of side-evaporative heat exchangers channels in livestock premises

**Abstract.** As a result of the numerical simulation of the indirect-evaporative air heat exchanger in the Star CCM+ software package, the distribution of the temperature field, the vector field of velocities and the absolute air humidity in channels of different shapes (square, equilateral triangle, circle) was established. The calculated coefficient of thermal efficiency of the heat exchanger with triangular channels is the whitest in contrast to the square and round forms.

**Streszczenie.** W wyniku symulacji numerycznej pośrednio-wyparnego powietrznego wymiennika ciepła w pakiecie Star CCM+ uzyskano rozkład pola temperatury, pola wektorowego prędkości oraz bezwzględnej wilgotności powietrza w kanałach o różnych kształtach (kwadrat, trójkąt równoboczny, koło) powstało. Obliczony współczynnik sprawności cieplnej wymiennika ciepła z kanałami trójkątnymi jest najbielszy w porównaniu do form kwadratowych i okrągłych (*Badanie strat ciśnienia i uzasadnienie kształtów kanałów bocznych wymienników ciepła w obiektach inwentarskich*)

**Keywords:** microclimate, livestock premises, ventilation, heat exchanger, parameters, research, dependencies. **Słowa kluczowe:** mikroklimat, wymienniki ciepła

### Introduction

Rapid growth of global power consumption in livestock complexes has caused serious concern about depletion of power resources. Increasing power consumption by animal husbandry complexes is caused by such factors as increasing number of animal populations and toughening requirements to microclimate maintenance in the premises [1].

The livestock sector of agro-industrial production has the greatest potential for increasing the efficiency of power use [2]. It can be seen that power used for air cooling represents a significant part of total power consumption, which is constantly growing due to increased requirements to optimal microclimate maintenance in livestock premises [3, 4, 5].

The largest share of the power consumption in animal husbandry premises falls on generation of standard microclimate parameters, in particular, on the heating of supply ventilation air. In the heating period, heat-generating devices of these premises consume, according to various estimates, from 40 to 90% of the total cost of fuel and power resources [1]. Therefore, even partial reduction of these costs will lead to a significant reduction in costs required for manufacture of animal husbandry products.

An effective way to reduce power consumption in livestock premises is to use the heat of ventilation emissions to heat supply ventilation air. The difficulty of using the air heat of ventilation emissions is that the exhaust air is a low-potential source of thermal power [6-9].

The most promising ways of using the heat of ventilation emissions are the use of heat exchangers (heat utilizers). Due to their efficiency, heat exchangers (heat utilizers) of ventilation emissions are becoming increasingly widespread both in residential and administrative premises, as well as in industrial buildings. The use of a heat exchanger (heat utilizer) of ventilation emissions in the system of microclimate maintenance in livestock premises allows reducing power consumption for supply air heating by up to 80% [10].

Over the past two decades, many new renewable power-based devices were introduced for the purpose of heating the agricultural industry premises: new heat recovery units, heat pumps, solar systems and many others

[11, 12, 13]. However, no renewable power-based devices have been widely applied in the field of cooling until now.

Automated ventilation system was created to remove air from piggery premises [14, 15, 16]. As a result of analytical studies of this system, the condition for its effective operation was mathematically represented [16, 17].

The factors causing difficulties in utilization of heat of ventilation emissions in livestock premises include [18-21]:

- significant air dustiness (up to 6 mg/cu m<sup>3</sup>);
- high air humidity in the premises, reaching 80% if standard parameters of air environment are observed;
- presence of high concentrations of aggressive gases in the air: ammonia – up to 20 mg/cu m<sup>3</sup>, hydrogen sulfide – up to 10 mg/cu m<sup>3</sup>, carbon dioxide – up to 0.28%;
- unacceptability of even partial recirculation of exhaust air for most livestock premises;
- significant amount of technological equipment, which is characteristic of modern animal husbandry premises and air exchange arrangement pattern determined thereby.

There are no such difficult conditions in whatever branch of national economy for use of heat exchangers (heat utilizers) as in agricultural production. Therefore, creation of workable and cost-effective designs of heat-utilizers for livestock premises, capable of being aggregated with a set of ventilation equipment, is a complex scientific and engineering task.

### Mathematical Foundation

Heat exchanger of the side-evaporative type have a system of channels, which is shown in Fig. 1. The heat exchanger contains independent working channels and connected wet and dry channels.

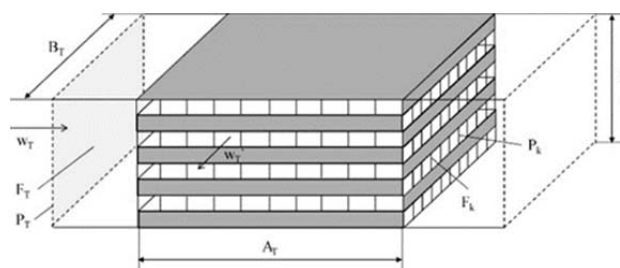


Fig. 1. Design diagram of side-evaporative heat exchanger P

Let's first consider the air flow through working channels. The air passes through three sections. The first section is distribution of air flow from large-diameter air duct into channels of a smaller diameter. Pressure losses are calculated using the formula

$$(1) \quad \Delta p_{Tk} = \eta_1 \left(1 - \frac{N_k F_k}{F_T}\right) \frac{\rho (w_T)^2}{2}$$

where  $\eta_1$  – is impact mitigation factor,  $\eta_1 = 0.5$  [22];  $N_k$  – number of channels;  $F_T$  – cross-sectional area of the inlet duct, sq m;  $F_k$  – cross-sectional area of the channel, sq m;  $w_T$  – is the average air velocity in working channels of side-evaporative heat exchanger.

The second section is air flow movement through the channels. Pressure losses are calculated using the formula

$$(2) \quad \Delta p_k = 0,11 N_k \frac{P_k A_T \rho w_T^2}{4 F_k} \sqrt{\frac{17 \mu_a P_k}{F_k \cdot w_k \cdot \rho} + \frac{\psi_k P_k}{4 F_k}}$$

Where  $P_k$  – is the perimeter of the channel section, sq m;  $A_T$  – the length of the working channel, sq m;  $\psi_k$  – equivalent roughness of the working channel walls [23, 24];  $\mu_a$  – dynamic air viscosity,  $\mu = 18.27 \cdot 10^{-6}$  N·s/sq m [25].

The third section is merging of the air flow from channels into the large-diameter duct. Pressure losses are calculated using the formula

$$(3) \quad \Delta p_{kT} = \eta_2 \left(1 - \frac{N_k F_k}{F_T}\right)^2 \frac{\rho (w_T)^2}{2}$$

Where  $\eta_2$  – is impact mitigation factor,  $\eta_2 = 0.5$  [23, 24].

The next step is to consider air movement through connected wet and dry ducts. At the same time, air passes through five areas. The first section is separation of air flow from the large-diameter air duct into channels of a smaller diameter. Pressure losses  $\Delta p_{Tk}$  are calculated using formula (1). The second section is air flow movement through dry channels. Pressure losses  $\Delta p_k$  are calculated using formula (2). The third section is pressure loss in a spatial (circular) turn by  $180^\circ$   $\Delta p_{k180}$  [18]

$$(4) \quad \Delta p_{k180} = \zeta_{k80} \frac{\rho (w_T)^2}{2}$$

Where  $\zeta_{k180}$  – is local resistance coefficient for the spatial (circular) turn by  $180^\circ$ , according to [23]  $\zeta_{k180} = 2$ .

The fourth section is air flow movement through wet channels. Pressure losses  $\Delta p_k$  are calculated using formula (2). The fifth section is merging of the air flow from the wet ducts into the large-diameter air duct. Pressure losses  $\Delta p_{kT}$  are calculated using formula (3).

Total pressure losses through side-evaporative heat exchanger are equal to the sum of the pressure losses in all the above-mentioned sections. Assuming the same number  $N_k$  and size (area  $F_k$  and perimeter  $P_k$ ) of working, dry and wet channels, we obtain a formula for calculation of air losses in side-evaporative air heat exchanger

$$(5) \quad \begin{aligned} \Delta \Delta p_T &= \Delta p_{Tk} + \Delta p_k + \Delta p_{kT} + \Delta p_{Tk} + \Delta p_k + \Delta p_{k180} \\ &\quad + \Delta p_k + \Delta p_{kT} = \\ &= \frac{\rho (w_T)^2}{2} \left[ \eta_1 \left(1 - \frac{N_k F_k}{F_T}\right) + 0,11 N_k \frac{P_k A_T}{4 F_k} \times \right. \\ &\quad \left. \times \sqrt{\frac{17 \mu_a P_k}{F_k \cdot w_T \cdot \rho} + \frac{\psi_k P_k}{4 F_k}} + \eta_2 \left(1 - \frac{N_k F_k}{F_T}\right)^2 \right] \\ &\quad + \frac{\rho (w_T)^2}{2} \left[ \eta_1 \left(1 - \frac{N_k F_k}{F_T}\right) + \right. \\ &\quad \left. + 0,11 N_k \frac{P_k B_T}{4 F_k} \sqrt{\frac{17 \mu_a P_k}{F_k \cdot w_T \cdot \rho} + \frac{\psi_k P_k}{4 F_k}} + \zeta_{k80} + \right. \\ &\quad \left. + 0,11 N_k \frac{P_k B_T}{4 F_k} \sqrt{\frac{17 \mu_a P_k}{F_k \cdot w_k \cdot \rho} + \frac{\psi_k P_k}{4 F_k}} \right. \\ &\quad \left. + \eta_2 \left(1 - \frac{N_k F_k}{F_T}\right)^2 \right] \end{aligned}$$

Where  $B_T$  – is the length of dry and wet channels, sq m;  $\psi_k$  – equivalent roughness of the walls of dry and wet channels [23];  $w_T$  – average air velocity in the dry and wet channels of side-evaporative heat exchanger, m/s.

Let's plot the dependence between pressure losses through side-evaporative heat exchanger  $\Delta p_T$  and the number of channels  $N_k$ , the channels' cross-sectional area  $F_k$ , the average air velocity in the channels under condition  $w_T = w_T$  and their shape (square, equilateral triangle, circle). To do this, we will use the dependence between perimeters of channels of different shapes and their area:

- square:

$$(6) \quad P_k = 4\sqrt{F_k}$$

- equilateral triangle:

$$(7) \quad P_k = 2\sqrt{F_k\sqrt{3}}$$

- circle:

$$(8) \quad P_k = 2\sqrt{\pi F_k}$$

Dependence (5) and calculated power required for air pumping through side-evaporative heat exchanger are calculated using the formula

$$(9) \quad N_{W1} = \frac{V \Delta p_T}{\eta_n}$$

Where  $\eta_n$  is total efficiency of the ventilator,  $\eta_n = 0.8$  [22] shown in fig. 2-3.

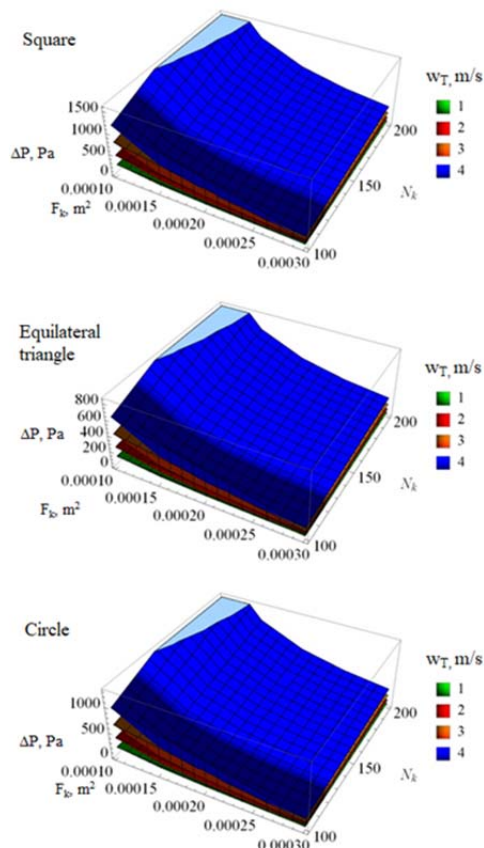


Fig. 2. Dependence between pressure losses  $\Delta p_T$  and the number of channels  $N_k$ , the channels' cross-sectional area  $F_k$ , the average air velocity in the channels under condition  $w_T = w_T$  and their shape (square, equilateral triangle, circle)

Analysis of fig. 2-3 allows stating that with the increase in the channels' cross-sectional area  $F_k$ , there occurs decrease in pressure losses  $\Delta p_T$  and power  $N_{W1}$ , which is required for air pumping through the side-evaporative heat exchanger. At the same time, the increase in the average air velocity in the channels  $w_T$  and their number  $N_k$  leads to the increase in pressure losses  $\Delta p_T$  and power  $N_{W1}$ . The

most effective form of channels (pressure loss reduction by 23%) in terms of pneumatic losses is an equilateral triangle.

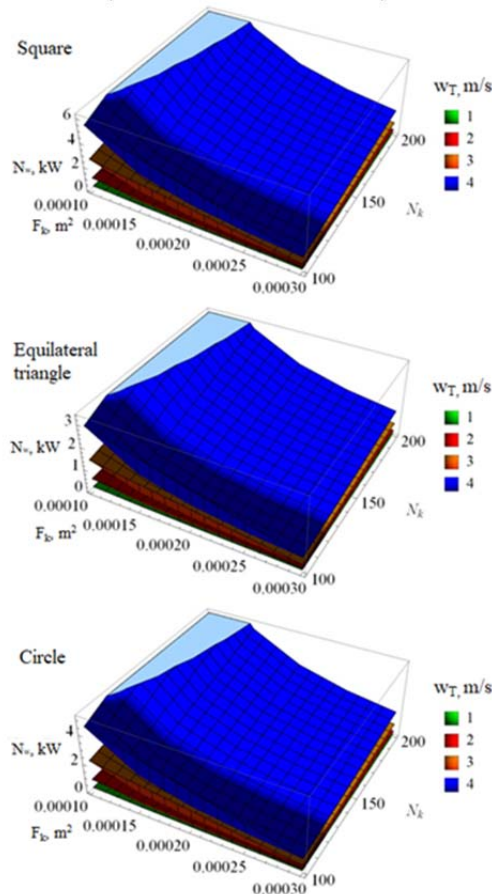


Fig. 3. Power  $N_{w1}$  dependence on the number of channels  $N_k$ , the cross-sectional area of the channels  $F_k$ , the average air velocity in the channels under condition  $w_T = w_T$  and their shape (square, equilateral triangle, circle).

### Numerical Methods

The main criteria for choosing recuperative heat exchangers (heat utilizers) are [11, 22]:

- thermal efficiency ratio, which is determined using formula [22, 25]:

$$(10) \quad \eta_t = \frac{T_{k2} - T_{n2}}{T_{n1} - T_{k1}}$$

Where  $T_{k2}$  – is the temperature of supply air at the outlet from the heat exchanger (heat recovery unit), °C;

$T_{n2}$  – is the temperature of supply (external) air at the inlet to the heat exchanger (heat utilizer), °C;

$T_{n1}$  – is the temperature of exhaust air at the inlet to the heat exchanger (heat utilizer), °C;

$T_{k1}$  – is the temperature of exhaust air at the outlet from the heat exchanger (heat utilizer), °C;

- sanitary and hygienic parameters: there should be no pollutants passing through the recuperator, it is necessary to ensure the possibility of controlling air quality and its purification to the greatest possible extent;

- power efficiency: this value characterizes specific power consumption, that is, how much the recuperative heat exchanger (heat recovery unit) consumes to return the unit of heat from removed air;

- operational characteristics: the structure must be suitable for repair, have a long service life, require minimal maintenance;

- structure cost.

To study the process of heat and mass transfer in a side-evaporative heat exchanger with different channel shapes, we will conduct numerical simulations in Star

CCM+ software package. As models for the continuum grid, the following were chosen: generator of polyhedral cells, generator of surface grid and extruder of cells. The basic size of a cell was 0.001 m, with maximum ratio of the sizes of connected mesh edges being 1.3. The layout of the channels and the general view of calculated grid of the side-evaporative heat exchanger are shown in fig. 4-6.

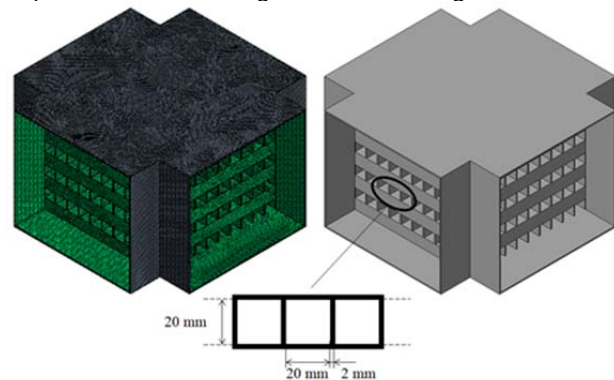


Fig. 4. Layout diagram of the channels and general view of calculated grid of side-evaporative heat exchanger with square channels

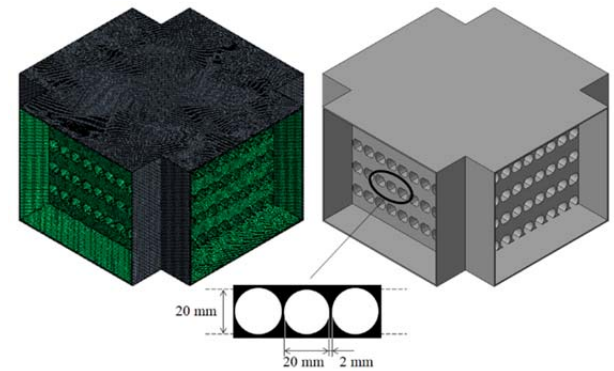


Fig. 5. Layout diagram of the channels and general view of calculated grid of side-evaporative heat exchanger with circular channels

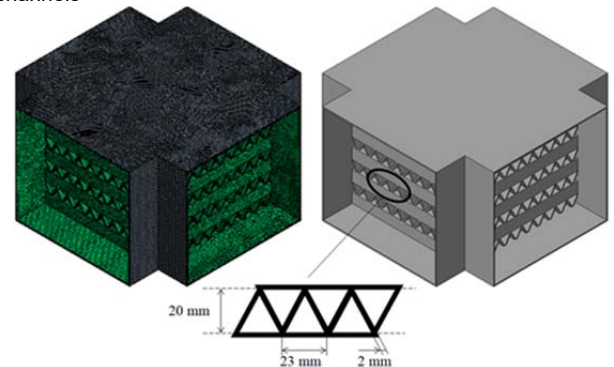


Fig. 6. Layout diagram of the channels and general view of calculated grid of side-evaporative heat exchanger with triangular channels

The following were chosen as physical models of dry and wet channels: three-dimensional, Eulerian multiphase model, method of separated flow and volume liquid VOF, model of phase interaction and model of separated multiphase temperature. The current flow was subjected to the Navier-Stokes equation and k-ε model of turbulence. The Euler phases were air and water. The air phase was subjected to MASVP-PR97 real gas (vapor) and turbulent flow models. The water phase was subjected to the Van der Waals real gas and turbulent flow models.

The following were chosen as physical models of the heat exchanger's walls: three-dimensional model of solid

body material, constant density, model of power of separated solid body.

Physiomechanical properties of all simulation phases are summarized in Table 1.

Table 1. Physiomechanical properties of modeling phases.

Property	Air phase	Water phase	Wall
Dynamic viscosity, Pa·s	$1.85508 \cdot 10^{-5}$	$1.26765 \cdot 10^{-5}$	-
Molecular weight, kg/mol	28.9664	18.0153	-
Thermal conductivity ratio, $V/(m \cdot K)$	0.0260305	0.0253325	0.44
Specific heat capacity, $J/(kg \cdot K)$	1003.62	1938,19	1700.0

Selected solver is of a stationary one. The number of internal inertias was equal to 10.

The dimensions of the side-evaporative heat exchanger and boundary conditions of modeling are shown in fig. 7. At the inlet to the heat exchanger, air flow was equal to  $Q_1 = Q_2 = 100 \text{ cu m/h}$ , the temperature was  $t_1 = 30 \text{ }^\circ\text{C}$ ,  $t_2 = 0 \text{ }^\circ\text{C}$ , absolute humidity –  $x_1 = x_2 = 5 \text{ g/kg}$ . Heat insulation is mounted around the heat exchanger, that is, heat exchange with the environment does not occur.

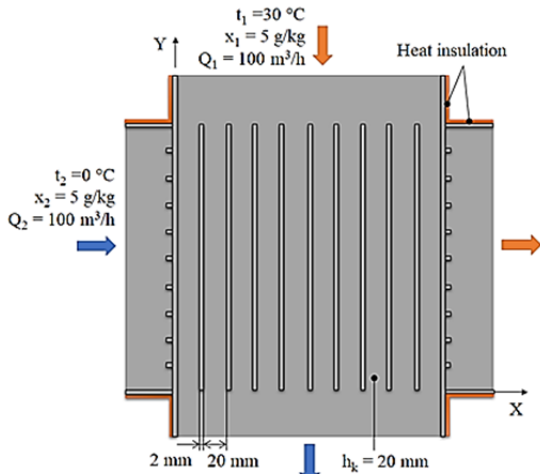


Fig. 7. Dimensions of the heat exchanger of side-evaporative cycle type and boundary conditions of modeling

## Results and Discussion

As a result of modeling, distribution of the temperature field in the heat exchanger with different channel shapes was obtained (see Fig. 8-13). Transverse distribution of the temperature field is characterized by formation of cylindrical velocity distribution in the middle of the channel, regardless of its shape. In turn, longitudinal distribution of the temperature field in side-evaporative heat exchanger shows the interaction between two air flows, which change their temperature due to heat conduction through the walls.

For square ducts, the temperature of the cold air flow varies on average from  $0^\circ\text{C}$  to  $10.3 \text{ }^\circ\text{C}$ , that of warm air – from  $0^\circ\text{C}$  to  $17.7^\circ\text{C}$ . Thermal efficiency ratio of the heat exchanger with square channels is  $\eta_t = 0.84$ .

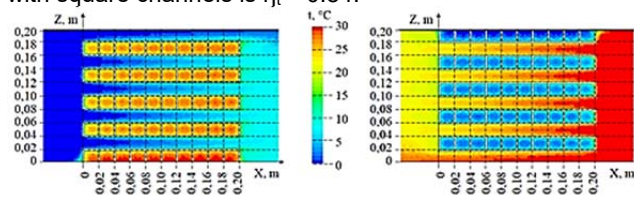


Fig. 8. Transverse distribution of the temperature field in side-evaporative heat exchanger with square channels

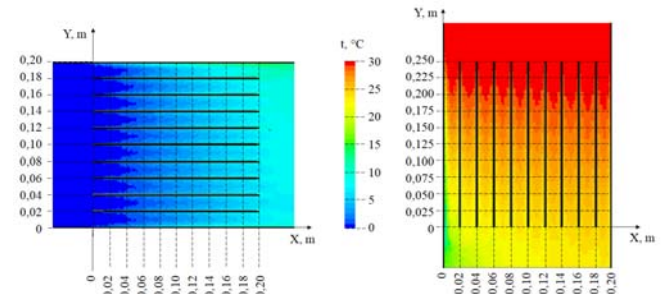


Fig. 9. Longitudinal distribution of the temperature field in side-evaporative heat exchanger with square channels

For round ducts, the temperature of cold air flow varies on the average from  $0^\circ\text{C}$  to  $9.4^\circ\text{C}$ , that of warm air – from  $0^\circ\text{C}$  to  $17.1^\circ\text{C}$ . Thermal efficiency ratio of the heat exchanger with circular channels is  $\eta_t = 0.73$ .

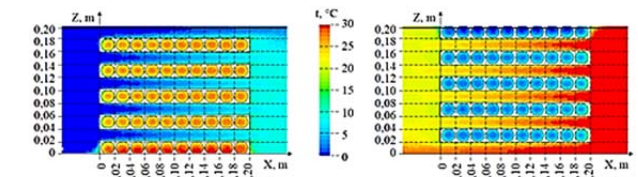


Fig. 10. Transverse distribution of temperature field in side-evaporative heat exchanger with circular channels

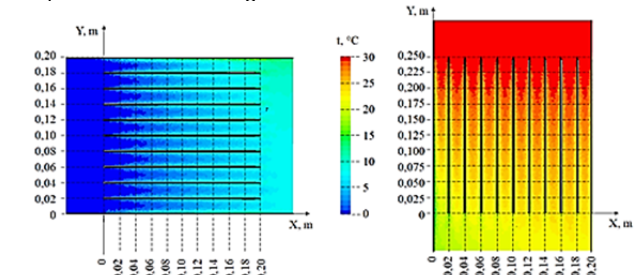


Fig. 11. Longitudinal distribution of temperature field in side-evaporative heat exchanger with circular channels

For triangular-shaped channels, the temperature of cold air flow varies on the average from  $0^\circ\text{C}$  to  $11.5^\circ\text{C}$ , that of warm air – from  $0^\circ\text{C}$  to  $18.2^\circ\text{C}$ . Thermal efficiency ratio of the heat exchanger with triangular channels is  $\eta_t = 0.97$ .

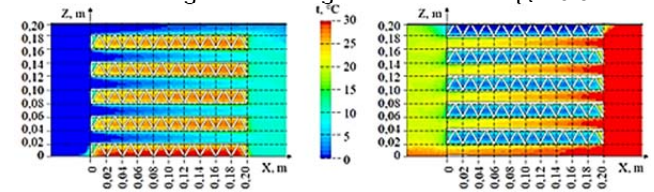


Fig. 12. Transverse distribution of temperature field in side-evaporative heat exchanger with triangular channels

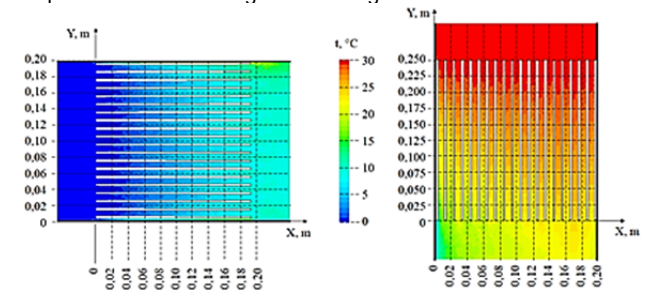


Fig. 13. Longitudinal distribution of temperature field in side-evaporative heat exchanger with triangular channels

To visualize the process of air flow movement through the channels of the heat exchanger, a vector field of velocities was constructed (see Fig. 14-16). Comparing the air flow distributions in all channels depending on their shape, we can conclude that for triangular channels, a more uniform air flow is observed over the entire cross-sectional area. The average speed is equal to  $V = 0.042$  m/s, with the ratio of its variation  $\delta_V = 0.88$ . At the same time, for square channels –  $V = 0.039$  m/s, and the ratio of variation  $\delta_V = 0.84$ , while for round channels –  $V = 0.046$  m/s, and the ratio of variation  $\delta_V = 0.81$ .

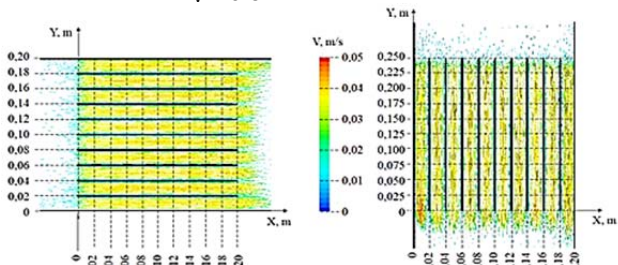


Fig. 14. Distribution of the velocity vector field in the side-evaporative heat exchanger with square channels

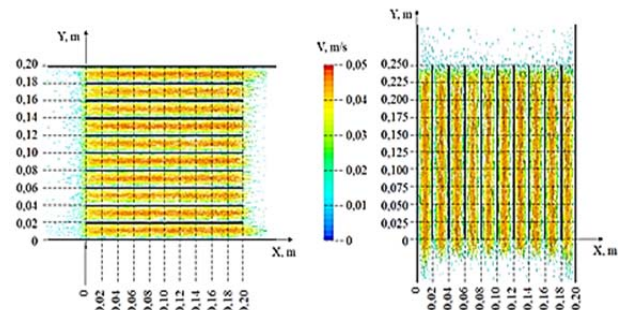


Fig. 15. Distribution of the velocity vector field in the side-evaporative heat exchanger with round channels

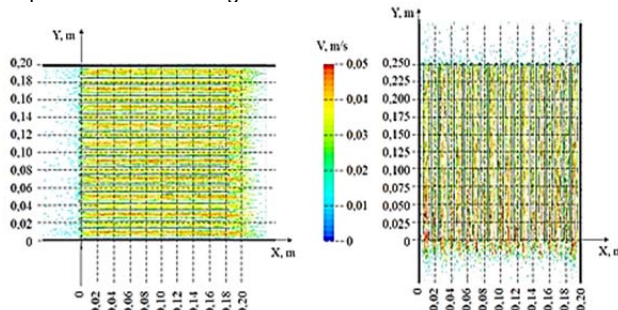


Fig. 16. Distribution of the velocity vector field in the side-evaporative heat exchanger with triangular channels

The change in air flow humidity during its movement is shown in fig. 17-19. During thermal air flow movement, a significant decrease in absolute humidity is observed to almost 0.01 g/kg. This is explained by the condensation phenomenon. Thus, cold air cools the walls of the heat exchanger. In turn, during warm air movement, the moisture contained in the flow turns into a liquid and settles on the cold walls of the heat exchanger. This phenomenon leads to decrease in the absolute humidity of warm air.

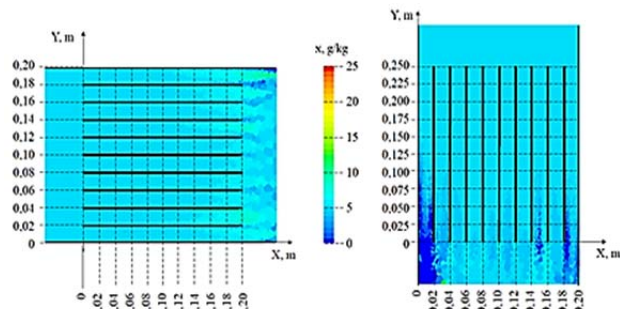


Fig. 17. Distribution of absolute air humidity in the side-evaporative heat exchanger with square channels

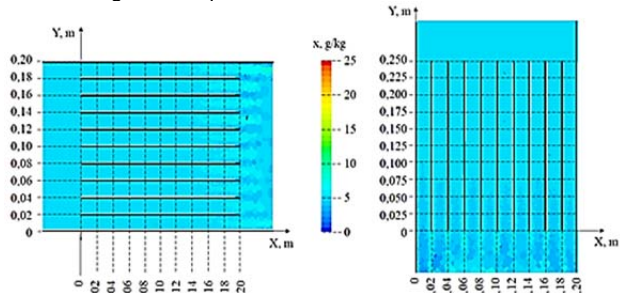


Fig. 18. Distribution of absolute air humidity in the side-evaporative heat exchanger with circular channels

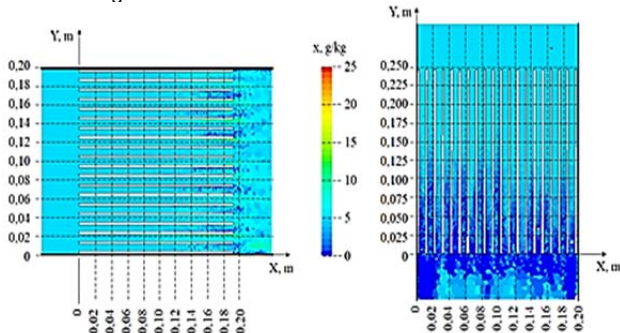


Fig. 19. Distribution of absolute air humidity in the side-evaporative heat exchanger with triangular channels

By comparing humidity distribution in channels of different shapes, one can state that decrease in the absolute humidity of thermal air flow sooner occurs in the side-evaporative type heat exchanger with triangular channels. This is evidenced by the data shown in Figure 19.

### Conclusion

As a result of analytical studies of pressure losses of an indirect-evaporative air heat exchanger, the dependences of pressure losses  $\Delta p_T$  and power  $N_T$  on the number of channels  $N_k$ , the cross-sectional area of channels  $F_k$ , the average air velocity in the channels under the condition  $w_T = w_T$  and their shape (square, equilateral triangle, circle). It was established that the most effective form of channels in terms of pneumatic losses (reduction of pressure losses by 23%) has channels in the form of an equilateral triangle.

As a result of the numerical simulation of the indirect-evaporative air heat exchanger in the Star CCM+ software package, the distribution of the temperature field, the vector field of velocities and the absolute air humidity in channels of different shapes (square, equilateral triangle, circle) was established.

The calculated coefficient of thermal efficiency of the heat exchanger with triangular channels is the biggest  $\eta_t = 0.97$ . For a square shape, it is  $\eta_t = 0.84$ , and for round –  $\eta_t = 0.73$ .

The average speed of the air flow in the triangular channels is  $V = 0.042$  m/s, and the coefficient of its variation is  $\delta_v = 0.88$ . In turn, for square channels –  $V = 0.039$  m/s, coefficient of variation  $\delta_v = 0.84$ , for round channels –  $V = 0.046$  m/s, coefficient of variation  $\delta_v = 0.81$ .

Comparing the humidity distribution in channels of different shapes, it can be stated that the decrease in the absolute humidity of the thermal air flow from 0.05 g/kg to 0.01 g/kg occurs earlier in the heat exchanger of the indirect-evaporative type with triangular channels.

The above statements make it possible to conclude that the indirect-evaporative air heat exchanger with triangular channels is the most efficient.

**Authors:** KALETNIK Hryhorii – *Dr. Sc. in Economics, Professor, Academician NAAS of Ukraine, Head of the Department of Administrative Management and Alternative Fuel Resources, Vinnytsia National Agrarian University* (21008, 3 Sonyachna str., Vinnytsia, Ukraine); YAROPUD Vitalii – *PhD in Engineering, Associate Professor, Dean of the Faculty of Engineering and Technology, Vinnytsia National Agrarian University* (21008, 3 Sonyachna str., Vinnytsia, Ukraine, e-mail: yaropud77@gmail.com).

#### REFERENCES

- [1]. Makarenko P.M., Kalinichenko O.V., Aranchiy V.I. Energy efficiency and energy saving: economic, technological and ecological aspects: collective monograph. *PP «Astraya»*, 2019, 603.
- [2]. Gunko I., Babyn I., Pryshliak V. Experimental studies of the air injector system operating modes of the milk washing system, *Scientific Horizons*, 3 (2021), 44–53.
- [3]. Gunko I., Hraniak V., Yaropud V., Kupchuk I., Rutkevych V. Optical sensor of harmful air impurity concentration. *Przegląd Elektrotechniczny*, 97 (2021), nr. 7, 76-79. <https://doi.org/10.15199/48.2021.07.15>
- [4]. Poberezhets Ju., Chudak R., Kupchuk I., Yaropud V., Rutkevych V. Effect of probiotic supplement on nutrient digestibility and production traits on broiler chicken, *Agraarteadus*, 32 (2021), nr. 2, 296-302. <https://doi.org/10.15159/jas.21.28>.
- [5]. Gunko I., Babyn I., Aliiev E., Yaropud V., Hrytsun A., Research into operating modes of the air injector of the milking parlor flushing system. *UPB Scientific bulletin, Series D: Mechanical Engineering*, 83 (2021), nr. 2, 297-310.
- [6]. Draganov B.H., Dolinskyi A.A., Mishchenko A.V., Pismennyi E.M. Heat engineering: textbook. *NKOS*, 2005, 504.
- [7]. Bozhenko M.F. Systems of heating, ventilation and air conditioning of buildings: education. *Kyiv: KPI named after Igor Sikorskyi*, 2019, 380.
- [8]. Paziuk V.M., Liubin M.V., Yaropud V.M., Tokarchuk O.A., Tokarchuk D.M. Research on the rational regimes of wheat seeds drying. *INMATEH – Agricultural Engineering*, 56 (2018), nr. 3, 39-48.
- [9]. Paziuk V.M., Petrova Zh.O., Tokarchuk O.A., Yaropud V.M. Research of rational modes of drying rape seed. *INMATEH – Agricultural Engineering*, 58 (2019), nr. 2, 303-310. <https://doi.org/10.35633/INMATEH-58-33>
- [10]. Borsch O.B. Energy saving in heat and gas supply systems, ventilation and air conditioning: training. *Poltava: PNTU*, 2009, 116.
- [11]. SOU 74.3-37-265:2005. Regenerative heat utilizers of ventilation emissions of livestock premises. Test methods. Ministry of Agrarian Policy of Ukraine, (2005), 38.
- [12]. Yaropud V. Analytical study of the automatic ventilation system for the intake of polluted air from the pigsty. *Scientific horizons*, 24 (2021), nr. 3. 19-27. [https://doi.org/10.48077/sciior.24\(3\).2021.19-27](https://doi.org/10.48077/sciior.24(3).2021.19-27)
- [13]. Spirin A., Kupchuk I., Tverdokhib I., Polievoda Yu., Kovalova K., Dmytrenko V. Substantiation of modes of drying alfalfa pulp by active ventilation in a laboratory electric dryer. *Przegląd Elektrotechniczny*, 98 (2022), nr. 5, 11-15. <https://doi.org/10.15199/48.2022.05.02>
- [14]. Kaletnik G.M., Yaropud V.M. Mechatronic system of microclimate provision of livestock premises, *Patent UA*, 148970 (2021).
- [15]. Yaropud V., Hunko I., Aliiev E., Kupchuk I. Justification of the mechatronic system for pigsty microclimate maintenance. *Agraarteadus*, 32 (2021), nr. 2. 212–218. <https://doi.org/10.15159/jas.21.21>
- [16]. Kaletnik G.M., Yaropud V.M. Physico-mathematical model of the ventilation system for injecting clean air in livestock premises. *Technology, energy, transport of agricultural industry*, 114 (2021), nr. 3, 4-15. <https://doi.org/10.37128/2520-6168-2021-3-1>
- [17]. Kaletnik G.M., Yaropud V.M. Simulation of the heat and mass transfer process of the indirect-evaporative type heat exchanger. *Technology, energy, transport of agricultural industry*, 116 (2022), nr. 1, 4-15. <https://doi.org/10.37128/2520-6168-2022-1-1>
- [18]. Kaletnik G.M., Yaropud V.M. Theoretical studies of pneumatic losses of the air heat exchanger of the indirect-evaporative type of livestock premises. *Machinery & Energetics*, 12 (2021), nr. 4, 35-41. <http://dx.doi.org/10.31548/machenergy2021.04.035>
- [19]. VNTP SGIp-46-5.97. Departmental norms of technological design. Animal and rabbit farms. Ministry of Agriculture and Production of Ukraine. *Noosphere*, (1994), 45.
- [20]. VNTP SGIp-46-4.94. Departmental norms of technological design. Poultry enterprises. Ministry of Agriculture and Production of Ukraine. *Noosphere*, (1994), 68.
- [21]. VNTP SGIp-46-2.95. Departmental norms of technological design. Pig farms. Ministry of Agriculture and Production of Ukraine. *Noosphere*, (1994), 68.
- [22]. DSTU 2921-94. Heating and ventilation units. Test methods. Approved and put into effect on January 1, 1996. State Committee for Standardization of Metrology and Certification of Ukraine, 42.
- [23]. Hasan A. Going below the wet bulb temperature by indirect evaporative cooling: Analysis using a modified  $\epsilon$ -NTU method. *Applied Energy*, 89 (2012), 237-245.
- [24]. Fedorets O.O., Salenko O.F. Hydraulics, hydraulic and pneumatic drive: textbook. 2nd ed., revised. and added. *Kyiv: Znannia*, 2009, 502.
- [25]. Yaropud V., Kupchuk I., Burlaka S., Poberezhets J., Babyn I. Experimental studies of design-and-technological parameters of heat exchanger. *Przegląd Elektrotechniczny*, 98 (2022), nr. 10, 57-60. <https://doi.org/10.15199/48.2022.10.10>